Insights into the Enantioselective Au(I)-Catalyzed Reactions between 2-Alkynyl Ketones and Naphthols using the TCDC Approach

Yunliang Yu, Meriem Daghmoum, Nazarii Sabat, Zhenhao Zhang, Gilles Frison, Angela Marinetti, Xavier Guinchard

Insights into the Enantioselective Au(I)-Catalyzed Reactions between 2-Alkynyl Ketones and Naphthols using the TCDC Approach

Yunliang Yu, [a,b] Meriem Daghmoum,[a] Nazarii Sabat,[a] Zhenhao Zhang,[a,c] Gilles Frison,[c,d,*]Angela Marinetti,[a,*] and Xavier Guinchard[a,*]

[a] Université Paris-Saclay, CNRS, Institut de Chimie des Substances Naturelles, UPR2301, 91198 Gif-sur-Yvette, France
angela.marinetti@cnrs.fr; xavier.guinchard@cnrs.fr.
[b] Université Paris-Saclay, CNRS, Institut de chimie moléculaire et des matériaux d'Orsay, 91405, Orsay, France
[c] LCM, CNRS, Ecole Polytechnique, Institut Polytechnique de Paris, 91128 Palaiseau, France
[d] Sorbonne Université, CNRS, Laboratoire de Chimie Théorique, 75005 Paris, France.
gilles.frison@cnrs.fr

Abstract. The CPAPhosAuCl bifunctional complexes catalyse the enantioselective tandem cycloisomerization-nucleophilic addition reactions between 2-alkynylenones and naphthols, where naphthols behave mainly as O-nucleophiles. The inherent acidity of the catalysts induces then the isomerization of the O-addition- into the C-addition products with concomitant decrease of their enantiomeric excesses. In depth mechanistic studies have provided insights into these processes. Subsequently, the undesired racemization pathways could be suppressed by using substituted naphthols as nucleophiles, which delivered a large series of chiral bicyclic furanes in high enantioselectivities.

Tandem cycloisomerizations/nucleophilic additions of 2-alkynyl enones have been largely investigated over the last twenty years, for the high structural diversity ~~of~~ that can be reached via these approaches. [1] Indeed, upon exposure of 2-alkynyl enones to certain □-acidic transition metals, a cycloisomerization occurs, giving a cationic furan type intermediate **A**. (Scheme 1, eq. 1). Seminal work from Larock[2] using $AuCl_3$ as the catalyst was followed by dozens of creative endeavors in the field, showing that the same cationic intermediates can be generated using a large range of transition metals and trapped by numerous nucleophiles or dipoles,[3] thus forming a variety of functionalized furans.[4] Enantioselective variants of these reactions have been reported, but enantiocontrol remain an issue that needs addressing in many cases.

Given the ionic nature of the key intermediate **A**, the stereocontrol of this class of reactions, might be achieved, at first sight, via either the Asymmetric Counterion-Directed Catalysis (ACDC) approach[5],[4f, h],[6] or the alternative Tethered Counterion Directed Catalysis (TCDC) approach that we have introduced recently.[7],[8]

The TCDC approach relies on a new family of bifunctional gold catalysts, the (CPAPhos)AuCl complexes, in which the gold atom is tethered to a chiral phosphoric acid function that generates *in situ* a phosphate counterion. We have demonstrated that tethering of gold to the phosphate counterion results in higher geometrical constraints, decreases the flexibility of the key intermediates, and finally improves the stereocontrol in selected catalytic reactions. These catalysts have been applied successfully to the dearomatization of naphthols with allenamides,[7b] as well as to the tandem cycloisomerization of 2-alkynyl enones / nucleophilic addition reactions (Scheme 1, eq. 2), using a variety of nucleophiles including indoles and nitrones.[7a, c]

In further studies, we have demonstrated that naphthols can also be used as nucleophiles in the same tandem reactions.[7d]

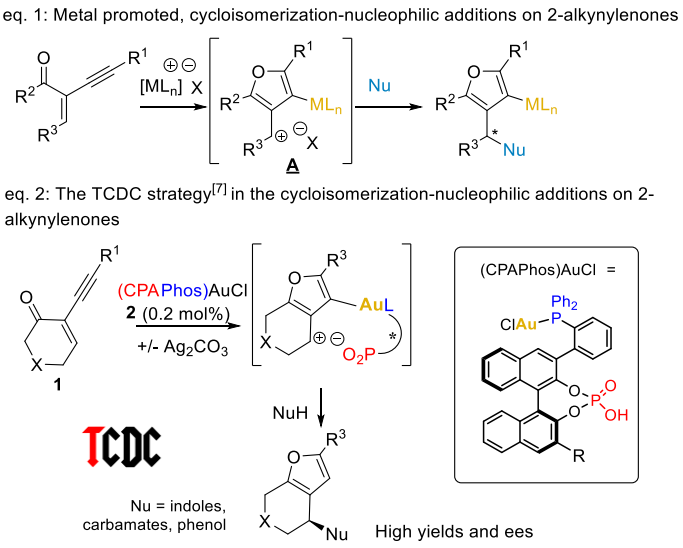

Scheme 1: Context of this study

These studies were inspired by the work of Xu and Ren on analogous reactions taking place under silver trifluoroacetate catalysis (Scheme 2, eq. 1).[9] They afforded oxidized compounds as the main products, resulting from the addition of naphthols as *C*-centered nucleophiles followed by *in situ* oxidation of the furan unit. A single attempt to run enantioselective variants using a chiral silver phosphate (AgTRIP), led to the final product in a moderate 42% ee.

Our own studies[7d] established that, under CPAPhosAuCl catalysis, 2-naphthols can behave as *O*-and/or *C*-nucleophiles[10] in their reaction with **1**, and that high enantioselectivities can be reached for both products **5** and **6** (Scheme 2, eq. 2), nicely complementing Ren's findings.[9] Importantly, the optimized conditions did not required the use of a silver salt for the activation of the catalyst. With all knowledge now available about the effect of the counter-ions in Au(I) catalysis[11] and the non-innocence role of the silver salt,[12] there is an undeniable importance of the development of silver-free strategies in Au(I) catalysis.[13],[14]

Eq. 1: Under Ag(I) catalysis (Xu and Ren)[9]

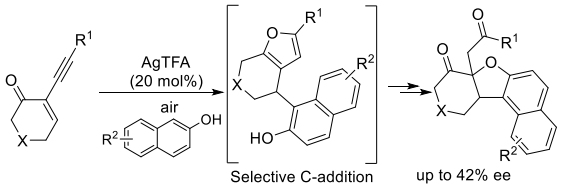

Eq. 2: Under Au(I) catalysis with the TCDC strategy[7]

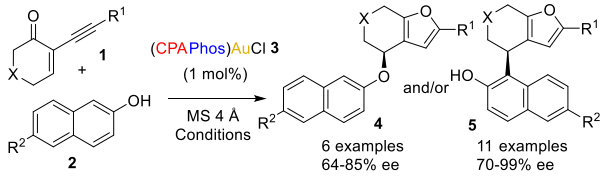

Scheme 2: Enantioselective tandem cycloisomerization /nucleophilic additions involving 2-alkynyl enones and 2-naphthols

However, the optimization of these reactions proved challenging, as far as their outcomes heavily depend on the catalysts used and the reaction conditions. The general trends that emerged from our catalytic tests are the following:

1. **The chemoselectivity is catalyst-dependent**. Catalyst **3a** (R=H, Scheme 3) favors the formation of *O*-addition products **4**, while catalyst **3b** (R = 3,5-bis(CF_3)C_6H_3) favors the *C*-addition compounds **5**.
2. **The stereochemical outcome of the reaction is solvent-dependent**. While reactions in DCM or DCE favor the formation of the (*S*)-enantiomers of **4**, reactions performed in ethereal solvents (Et_2O, MTBE…) favor the formation of (*R*)-**4**.
3. **The *O*-addition product 4 is structurally unstable and converts to C-addition product 5. Compounds 4 are also configurationally unstable under the conditions of the catalytic reactions.** Both processes impose very short and controlled reaction times.

This last point in particular led us to consider mechanistic issues in more depth. In this paper, we disclose detailed mechanistic studies and report on the extension of the synthetic approach to a large number of 1- and 2-substituted naphthols nucleophiles that enable to overcome the structural and configurational instability of these products.

A number of experiments were designed and performed in order to enlighten the above time-dependence of product ratios and ees. At first, a sample of the *O*-addition product (*S*)-**4a** (90:10 er) was exposed to 1 mol% of the chiral catalyst (*S*)-(CPAPhos^{A})AuCl **3a** in DCM at rt and the mixture was monitored by ^{1}H NMR and chiral HPLC over 1h timespan (Scheme 3, eq. 1). Compound **4a** evolved over the time into the *C*-addition product **5a**, reaching an approximate 65/35 ratio after 1 h. The enantiomeric ratio of (*S*)-**4a** decreased concurrently from 90:10 to 67.5:32.5. The *C*-addition product (*S*)-**5a** was formed initially with a 89:11 er that decreased slightly over the time. The same trend was observed using (*S*)-(CPAPhos^{B})AuCl **3b**, with an even faster process (Scheme 3, eq. 2). Exposure to this catalyst results in a higher **4a** to **5a** conversion rate and a faster decrease of the er over the time.

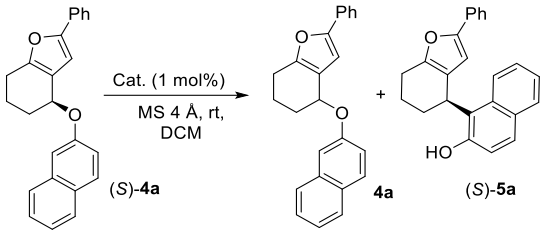

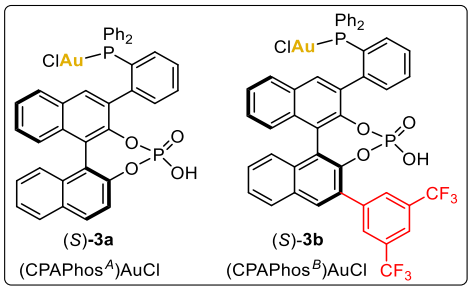

Eq.1: Cat = CPAPhos^{A}AuCl

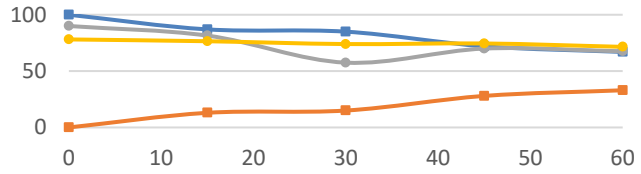

Eq. 2: Cat = CPAPhos^{B}AuCl

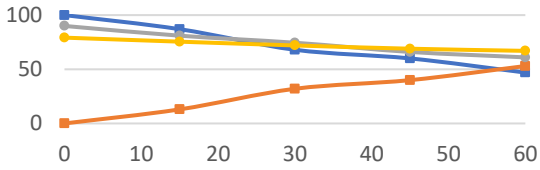

Eq. 3: Cat = CPAPhos^{B}AuCl + Ag_2CO_3

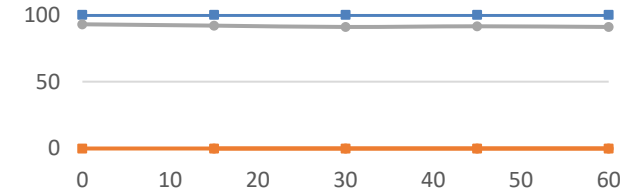

Eq. 4: Cat = *rac*-BINOL hydrogen phosphate (5 mol%)

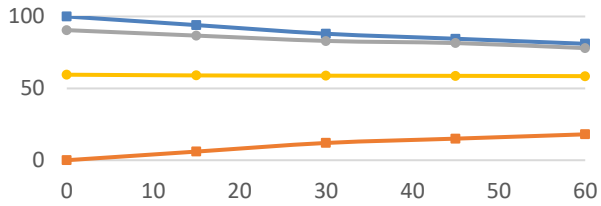

Eq. 5: Cat = CPAPhos^{B}AuCl + Ag_2CO_3, with excess 2-naphthol

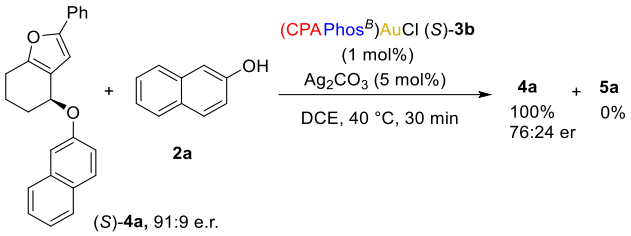

Eq. 6: Cat = AgTFA with/without excess 2-naphthol

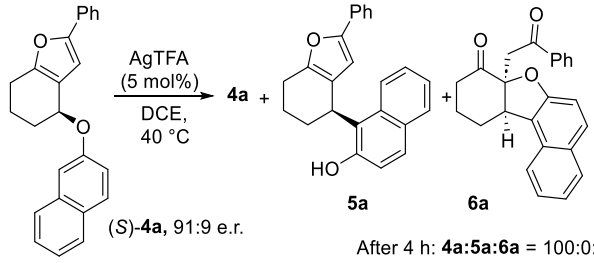

After 4 h: **4a:5a:6a** = 100:0:0
With 2-naphthol, after 4 h: **4a:5a:6a** = 40:13:37

Eq. 7: Cat = CPAPhos^{B}AuCl. Reaction carried out on (*R*)-**4a**

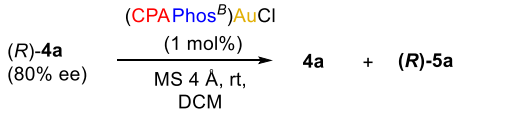

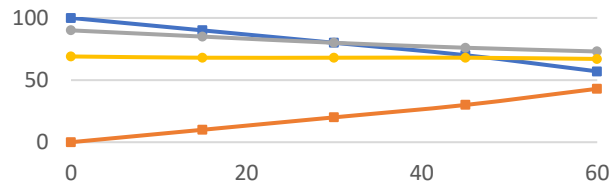

Eq. 8: Cat = CPAPhos^{B}AuCl. Reaction carried out on *rac*-**4a**

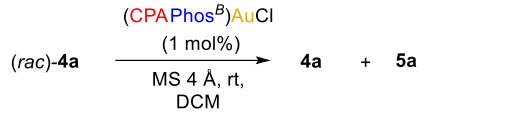

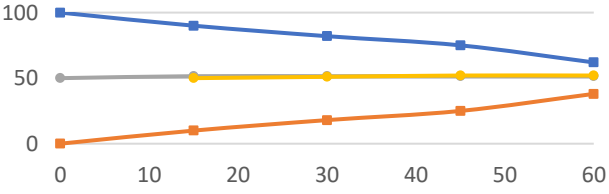

Scheme 3: Control experiments on the structural and configurational stability of 4a[a] Key molar fraction of **4a**.

■ molar fraction of **5a**. ● (*S*)-**4a**/(*R*+*S*)-**4a** ratio. ● (*S*)-**5a**/(*R*+*S*)-**5a** ratio (data at t= 0 min are extrapolated values).

On the contrary, when enantioenriched (*S*)-**4a** was treated with the same chiral catalyst (*S*)-**3b**, in the presence of Ag_2CO_3, the starting (*S*)-**4a** remained untouched (eq. 3). This experiment suggests that the phosphoric acid function of the (CPAPhos)AuCl catalyst is likely to be responsible for the whole process. This was confirmed by exposing **4a** to the acidic 1,1'-binaphthyl-2,2'-diyl hydrogenphosphate (Scheme 3, eq. 4), which elicited both conversion of **4a** into **5a** and stereochemical erosion of **4a**, that took place however at a lower rate than with (CPAPhos)AuCl (eq.4 vs eq. 1 and 2), as a result of the respective pKa values.

Interestingly, additional control experiment have shown that the concurrent use of CPAPhosAuCl and silver carbonate in the presence of an excess of naphthol (which are the actual reaction conditions) restore the racemization pathway (Scheme 3, eq. 5). The combined detrimental effects of the acidic function of the catalyst and the excess naphthol explain why short reaction times are necessary to obtain 4 in high ees, under the conditions of the catalytic process.

When compound **4a** was exposed to AgTFA (conditions of Ren[9]), it was found configurationally unstable over a four hours timespan (Scheme 3, eq. 6, 76:24 er for **4a**, and Fig S1). When the same experiment was performed in the presence of 2-naphthol, **4a** showed structural and configurational instability (71:29 er for **4a** after 4 h, eq. 6 and Fig S2) as in the case of the eq. 5, generating **5a** with the gradual concomitant formation of the oxidized product **6a**. When the whole process, i.e. the reaction between **1a** and **2a** catalyzed by AgTFA, was monitored, we found that the reaction is actually complete after 30 min, leading to the major formation of the *O*-addition product **4a** and evolving over the time to the *C*-addition and oxidation products (Fig S3). This demonstrates that the actual product of the silver-catalyzed reaction is not the C-addition product **5a** but instead the ether **4a** that further evolves to compound **5a.** This rearrangement requires the presence of 2-naphthol in an at least catalytic amount.

We next exposed the (*R*)-enantiomer of **4a** to complex (*S*)-**3b** for 1 hour and observed a decrease of the er from 90:10 to 73:27, while (*R*)-**5a** was formed with a 67:33 er (Scheme 3, eq. 7). This demonstrates that the (*R*)-enantiomer of the substrate **4a** undergoes slower isomerization with respect to the (*S*)-enantiomer (eq. 1 vs eq. 7), along with a lower racemization rate.
Under the same conditions, *rac*-**4a** produced nearly racemic **5a**, showing that the stereochemical control does not arise from the chiral Au(I) catalyst (*S*)-**3a**, but mainly from a chirality transfer from the substrate (Scheme 3, eq. 8).
The transfer of chirality from **4a** to **5a**, which can be estimated from the extrapolated initial er value of **5a**, is higher when using (*S*)-**4a** (about 86%) than using (*R*)-**4a** (about 76%). This demonstrates a certain degree of match effect between (*S*)-**4a** and the (*S*)-configured catalyst and mismatch effect between (*R*)-**4a** and the (*S*)-catalyst. The ee of the formed **5a** drops slightly over the time in both cases.

This batch of experiments has clearly established the instability of the *O*-addition products under acidic conditions. On the contrary, a sample of enantioenriched *C*-addition product (-)-**5a** remained unchanged in the presence of the acidic (CPAPhos)AuCl catalyst (See Fig S4), demonstrating its configurational and structural stability under these conditions.

Another experiment provided crucial information. Compound **4a** was reacted with 1-naphthol **2b** in the presence of complex (*S*)-**3b** and the composition of the mixture was monitored by ^{1}H NMR over 2.5 h (Scheme 4). It was found that after 30 min, the mixture contained only 23% of the starting material and 38% of the *C*-addition product **5a**, together with the two 1-naphthol derived compounds **4b** (23%) and **5b** (16%). Both *O*-addition products **4a** and **4b** virtually disappeared after 2.5 h, in favor of the formation of the corresponding *C*-addition products **5a** and **5b**. These results attest for a reaction pathway involving cleavage of the C-O bond of the starting material **4a**. It also clearly established that the O-add product **4b** resulting from the addition of 1-naphthol possesses the same structural instability than that of **4a**.

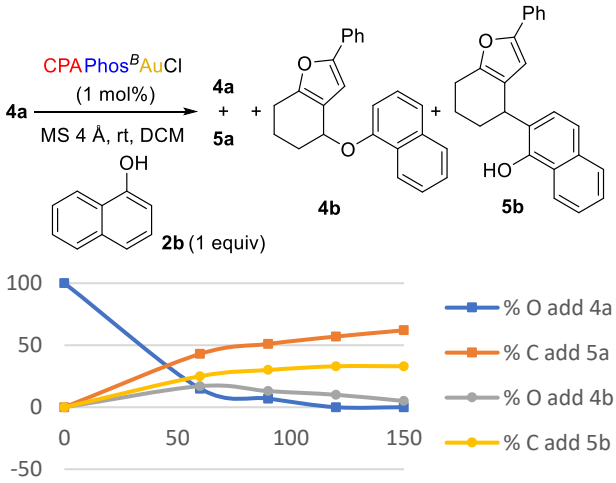

Scheme 4: Evidence for an intermolecular exchange process by cross experiments

On the basis of the catalytic tests in ref. 7d and the control experiments above, we pictured a plausible mechanism accounting for the outcomes of the catalytic reactions, including the erosion of the enantiomeric excess of compound **4a** and its conversion into **5a** (Scheme 5). These mechanistic issues are outlined hereafter.
First, both products **5a** and **4a** are formed initially with high enantioselectivity from the Au-promoted reaction (high ees for short reaction times). The absolute configuration of the final products (*S*)-**4a** and (*S*)-**5a** should be determined by the preferred conformation of

intermediate ***i*** that is formed in the cycloisomerization step. As shown in our previous reports,[7a, c] the lowest energy form of the intermediate carbocation ***i*** features a free pro-(*S*) face where the naphthol nucleophile will add preferentially.
However, compound **4a** can be H-bonded by the acidic catalyst (CPAPhos)AuCl **3**, as in intermediate ***ii***. Intermediate ***ii*** evolves then into intermediate ***iii*** by weakening the C-O bond and transferring the proton to the naphthol unit. Our experiments indicate that two different pathways are then operating concurrently (as supported by eq. 1 and 2 in Scheme 3): (1) the reversible cleavage of the C-O bond that promotes racemization of the *O*-addition product **4a** and (2) the intramolecular formation of the *C*-addition product, that proceeds with partial chirality transfer and leads to enantioenriched, (*S*)-configured **5a**. The chiral gold catalyst does not provide any significant chiral induction at this step, as shown by the experiment on racemic **4a** (eq. 8, Scheme 3). Compound **5a** is configurationally stable, nevertheless decrease of the ee over the time results from the erosion of the ee of its precursor **4a**.

To gain better insight into the erosion of the enantiomeric excess and the instability of the *O*-addition products **4**, we have carried out a computational study at the DFT level (see SI for details). We have considered the reaction between compound (*S*)-**4a** and the BINOL-derived chiral phosphoric acid (*S*)-**3c** (Figure 1), as a model of the phosphoric acid unit of (*S*)-**3a**, as we have shown that the racemic form of **3c** catalyzes the same rearrangement and partial racemization (see Scheme 3, eq. 4). We have first computed a pathway that reasonably explains the rearrangement. Compound **4a** binds to **3c** through *H*-bonding, forming **7a**. This complex can evolve, via breaking of the C-O bond and proton transfer to form pro-(*S*)-**8a**. This carbocationic intermediate retains the initial stereochemical information, due to the interaction between the naphthol oxygen and the cationic site. **8a** can then change its geometry. In particular, the naphthol and the cyclic cationic moieties, both approximately planar and located in parallel planes, can shift relative to each other, leading to pro-(*S*)-**9a** where the cationic site interacts preferentially with the electron-rich carbon of the naphthol. **9a** retains the chiral information present in **4a**. The formation of the C-C bond followed by re-aromatization of the naphthol moiety leads to (*S*)-**5a** in 2 steps from **9a**.
Overall, the conversion of **4a** to **5a** is exothermic by 22.9 kJ/mol, which explains the irreversible formation of the *C*-addition product. However, the activation barrier of this process is high (107.6 kJ/mol from **7a**), which explains why the conversion of **4a** into **5a** upon exposure to the acidic catalyst is slow.[15]

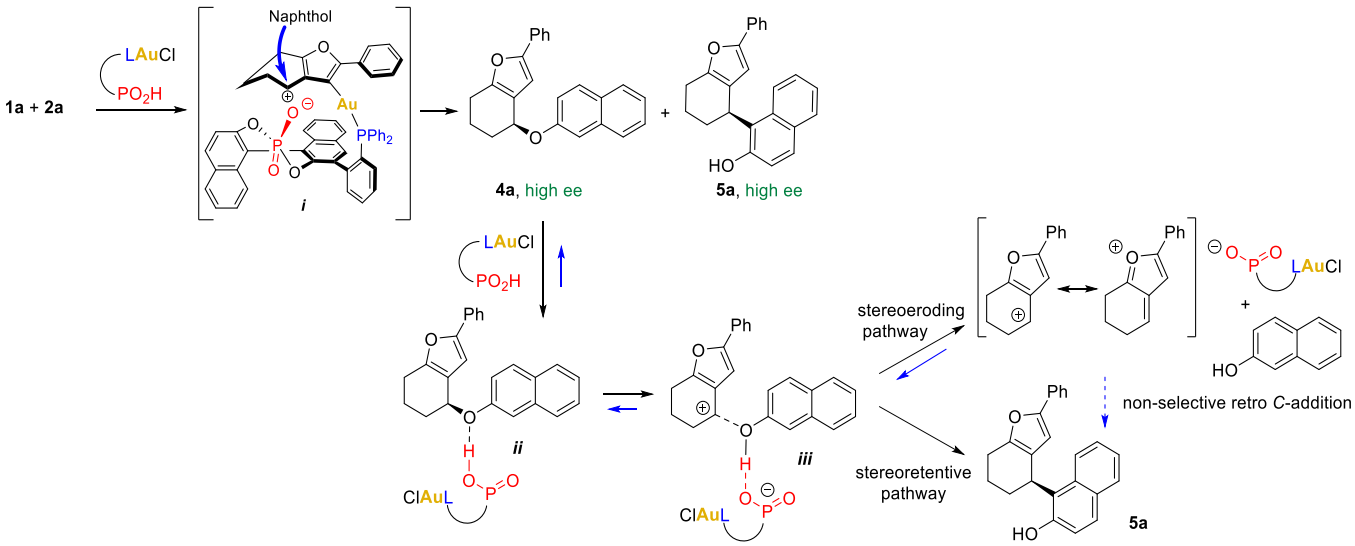

Scheme 5: Proposed pathways for the epimerization of **4a** and the conversion of **4a** into **5a.**

Figure 1. Schematic potential energy surface (Gibbs free energy in kJ mol^{-1}) for the conversion of the *O*-addition product **4a** into the C-addition product **5a**, calculated at the IEFPCM(DCM)-M06/Def2-TZVPP//IEFPCM(DCM)-M06/Def2-SVP level.

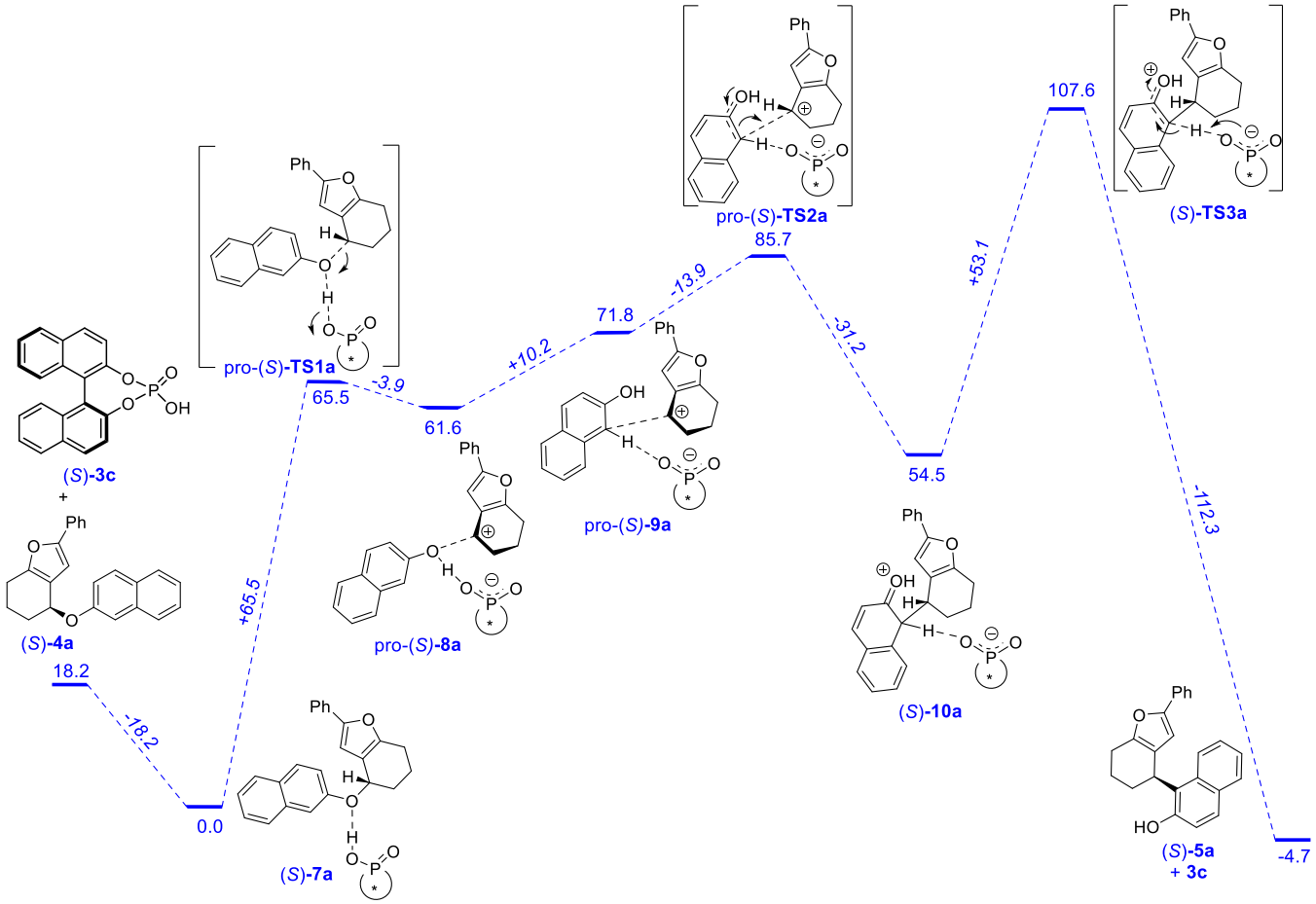

Figure 2. Schematic potential energy surface (Gibbs free energy in kJ mol^{-1}) for the erosion of the stereochemical information of **4a** obtained at the IEFPCM(DCM)-M06/Def2-TZVPP//IEFPCM(DCM)-M06/Def2-SVP level.

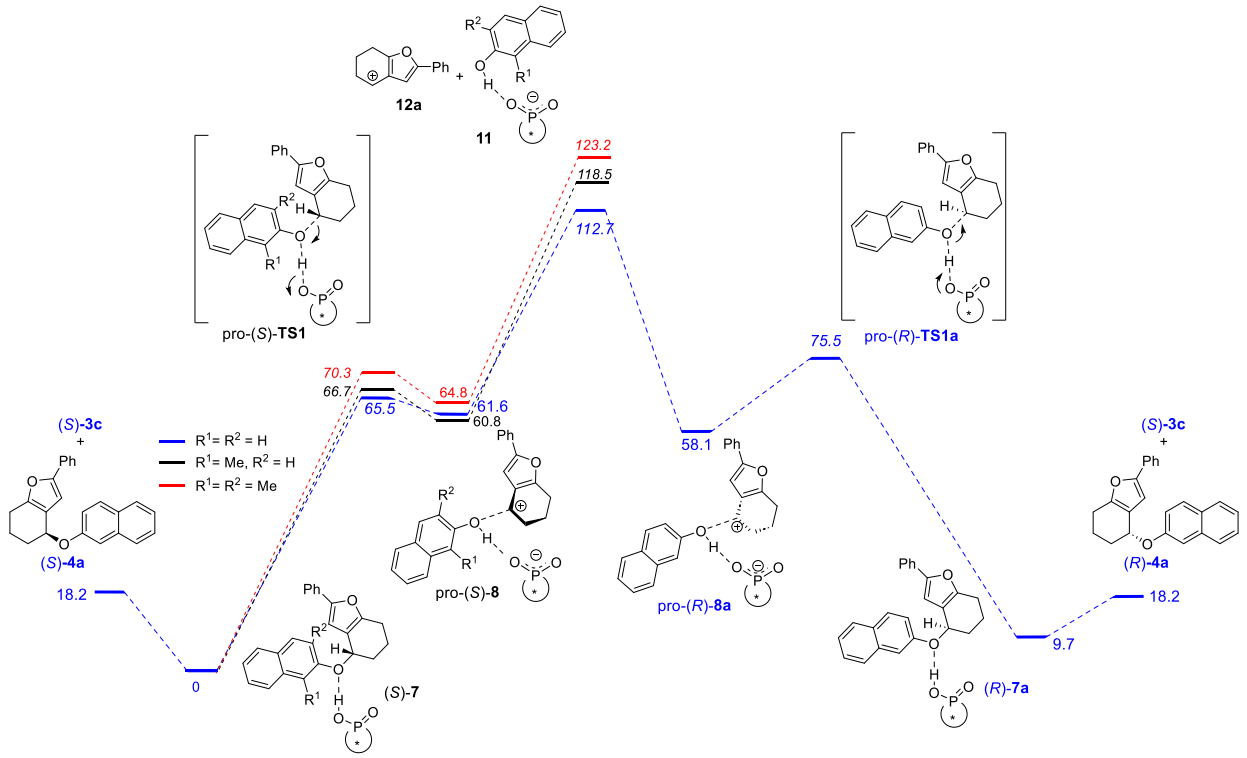

In a second step, the drop of the enantiomeric excess of **4a** has been tackled by DFT (Figure 2). Although dissociation of the ion pair **8a** into its separated ions **12a** + **11a** is highly endothermic (112.7 kJ/mol from **7a**,

51.1 kJ/mol from intermediate **8a**), at room temperature the barrier remain accessible. The stereochemical information is lost in carbocation **12a** and the subsequent *O*-addition of naphthol can take place from both faces, leading back to pro-(*S*)-**8a** or to pro-(*R*)-**8a**. The two intermediates then readily lead to the *O*-addition product **4a** with either (*S*) or (*R*) configuration. The energy levels of the two intermediates (*R*)- and (*S*)-**8a** are sufficiently different (= 3.5 kJ/mol) to account for the slight difference in the racemization rates observed for (*S*)-**4a** and (*R*)-**4a**.

As shown in Figure 1, DFT calculations confirm that the rearrangement of **4** to **5** retains the chiral information. Nevertheless, under the conditions of the catalytic reactions, the ees of both products decrease over the time, due to the slow racemization of **4**. We therefore hypothesized that this drawback might be overcome by using *ortho*-mono- or disubstituted naphthols. In this case, the energy barrier for the dissociation of the C-O bond should be higher because of an increased steric hindrance around the naphtyl ether moiety. Moreover, the formation of C-addition products should be either disfavored or totally prevented. To validate this hypothesis, the conversion of **4** to **11** has been investigated by DFT, starting from the 1-methyl-2-naphthyl ether **4h** and the 1,3-dimethyl-2-naphthyl ether **4c**, which possess one or two methyl groups at the ortho/ortho' positions of the ether functions (Figure 2, red and black traces and Table 1).
Contrary to our expectation, it appeared that the electronic effect of the methyl groups has a greater influence on C-O cleavage than their steric hindrance. DFT calculations have evidenced indeed a stronger H-bonding between **4h**/**4c** and the phosphoric acid **3c** compared to **4a** (26.6/34.9 *vs* 18.2 kJ/mol). This increased stabilization of **7h** and **7c** relative to **7a** is not offset by a less endergonic cleavage of the C-O bond leading to **8** (60.8, 64.8 and 61.6 kJ/mol for **7h**,**7c** and **7a**, respectively). Moreover, the electrostatic interaction within the ion pair **11**+**12** is slightly strengthened by the presence of methyl groups (energy barriers from **8** to **11** = +57.7/+58.4 *vs* +51.1 for **11h**/**11c** *vs* **11a**). Thus, the energy required from **7** to obtain a dissociated ion pair **11**+**12** increases from 112.7 kJ/mol (**7a**) to 118.5 (**7h**) and 123.2 kJ/mol (**7c**). Such an increase corresponds to a reaction rate decrease by a factor of 10 to 70, indicating that a double substitution on 2-naphthol by ortho-donating groups should significantly slow down the racemization, allowing the experimental achievement of a high enantiomeric excess.

Table 1: Computed relative Gibbs free energy[a] for the epimerization process of **4a**, **4h** and **4c**

entry	**4**[b]	**7**	**TS1**	**8**	**11**[c]	k_{rel}[d]
a	+18.2	0.0	+65.5	+61.6	+112.7	1
h	+26.6	0.0	+66.7	+60.8	+118.5	10.5
c	+34.9	0.0	+70.3	+64.8	+123.2	69.4

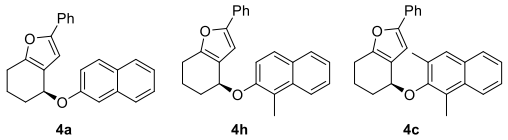

[a] Energy in kJ/mol at the IEFPCM(DCM)-M06/Def2-TZVPP//IEFPCM(DCM)-M06/Def2-SVP level. [b] Including catalyst **3c**. [c] Including cation **12a**. [c] Relative rate constants in $M^{-1}.s^{-1}$.

Based on this hypothesis, we have designed a new series of catalytic experiments that involve a range of 1,3-disubstituted and 1-substituted 2-naphthols as nucleophiles. The reaction conditions have been optimized using the phenylethynyl-cyclohexenone **1a** and 1,3-dimethyl-2-naphthol **2c** as the substrates (Table 2).

Table 2: Optimization of the reaction between **1a** and 1,3-dimethyl-2-naphthol **2c**

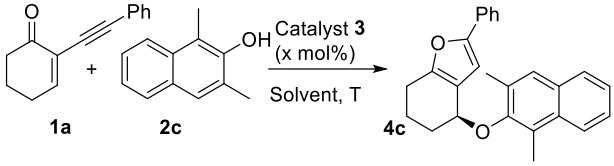

entry	catalyst	solvent	T °C	yield **4c** (%)[a]	ee **4c** (%)[b]
1[c]	**3a** (1)	DCM	rt	90	66
2[c]	**3b**(1)	DCM	rt	68	86
3	**3b** (1)	DCM	rt	65	87
4	**3b** (1)	DCM	0	99	90
5	**3b** (1)	DCM	-10	44	90
6	**3b** (0.2)	DCM	0	94	88
7	**3b** (0.2)	PhMe	0	92	91
8[d]	**3b** (0.2)	PhMe	0	93	95

[a] Isolated yields. [b] Enantiomeric excesses were measured by chiral HPLC. [c] Reactions performed in the presence of Ag_2CO_3 (0.5 mol%). [d] Reaction performed at 0.1 M. Most reactions were complete over 1.5 h, except entries 5-8 complete over 5 h.

The reactions were carried out initially in DCM, at rt, using 1 mol% of (CPAPhos^A)AuCl **3a**[7a] or (CPAPhos^B)AuCl **3b**,[7c] in the presence of 0.5 mol% of silver carbonate. Catalyst **3a** delivered the bicyclic furan **4c** in 90% yield and 66% ee (entry 1), while catalyst **3b** led to a significantly improved 86% ee (entry 2). With catalyst **3b,** the reaction could be carried out also in the absence of silver carbonate, with similar levels of catalytic activity and enantioselectivity (entry 3 vs 2), confirming the stability of product **4c** in the presence of the acidic catalyst. This shows that the

dissociation step, after protonation of the naphthyl ether **4c** is energetically demanding, as suggested by the DFT calculations above. After further optimization of the reaction temperature (0 °C), solvent (toluene) and concentration (0.1 M), the desired product **4c** was obtained in excellent yield (93%) and ee (95% ee), at the extremely low catalyst loading of 0.2 mol% (entry 8).

The scope of the reaction was investigated then under the optimized conditions above, using (CPAPhos^{B})AuCl **3b** (0.2 mol%) as the catalyst, with both di- and mono-substituted 2-naphthols as nucleophiles (Scheme 6). Starting from 2-naphthols with different combinations of methyl, ethyl and benzyl groups as R^2/R^3 substituents, the reaction afforded **4c-g** in excellent enantioselectivities (>93% ee). Monosubstituted naphthols (R^3=H) with methyl, ethyl and acetyl R^2 groups generated **4h-j** in high yields and enantioselectivities (86-93% ee). However, a benzyl group led to a drop of the enantiomeric excess (**4k**, 22% ee).

Next, the catalytic screening has been extended to the reactions between the alkynyl ketone **1a** and various 2-substituted 1-naphthols. The 2-Me, allyl and *n*-Pr substituted naphthols **2**, resulted in the formation of **4l-n** in high yields (66-92%) and enantioselectivities (80-87% ee). This showed that 1-naphthols may be suitable substrates also, although they give slightly lower ees than 2-naphthols.

In a second series of experiments, the yne-enone substrates **1** were varied. The R^1 group was changed from phenyl to both substituted aryls and alkyl groups. Some of these substrates required the use of silver carbonate to increase the level of enantioselectivity and/or the conversion rate. The reactions of naphthol **2c** with *p*-chlorophenyl- and *p*-tolyl-substituted yne-enones **1b** and **1c** proceeded smoothly and delivered **4o** and **4p** with 96% ee, in the presence of silver carbonate, while without the silver activator no/low conversion rates were observed.

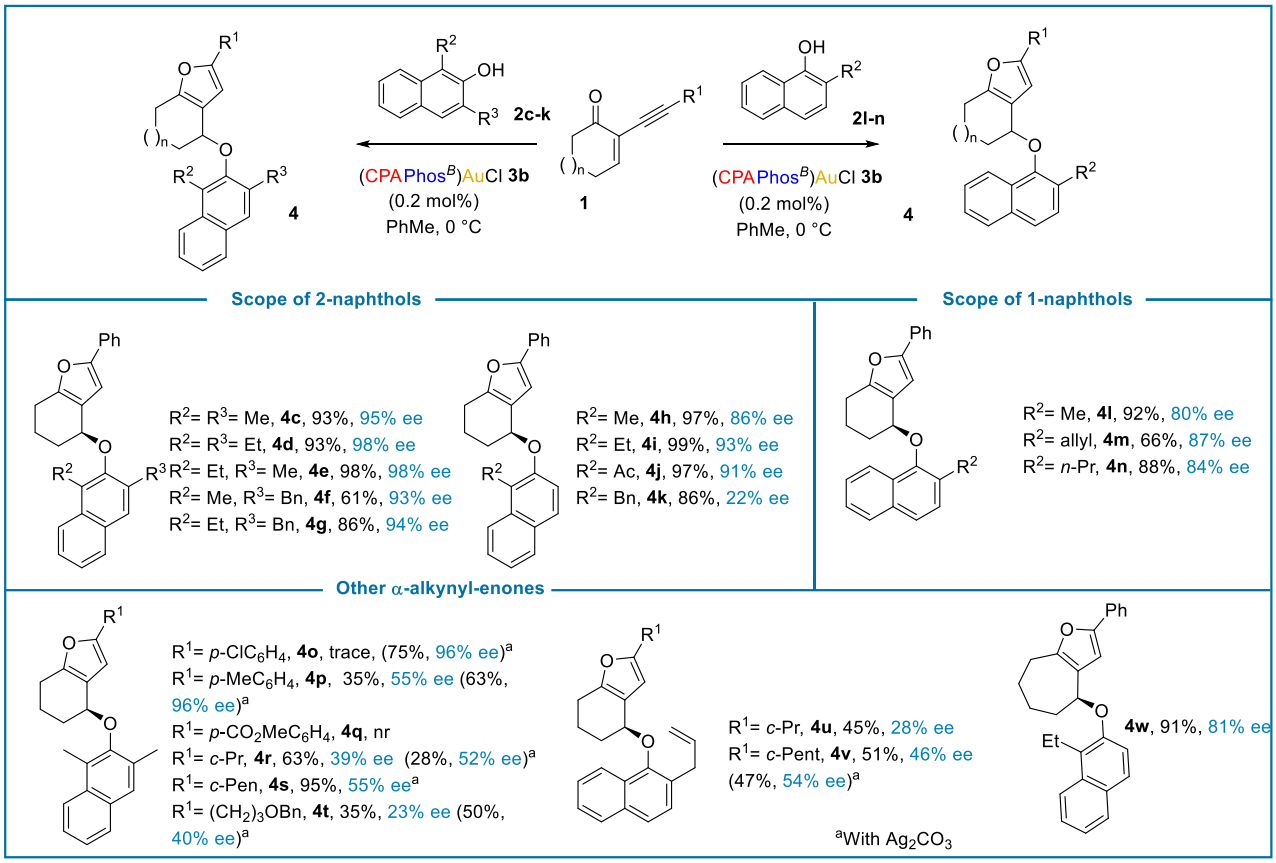

Scheme 6: Reactions of cyclic □-alkynyl-enones with substituted 1- and 2-naphthols

The introduction of an ester group on the phenyl substituent deactivates totally the substrate and therefore the starting material remains intact, both in the presence or absence of silver carbonate. For R^1 = alkyl, the reaction with the 2-naphthol **2c** led to compounds **4r-t** in good yields, but only moderate enantioselectivity (39-55% ee). Similarly, moderate ees were obtained from the reactions of alkyl-substituted enones with 2-allyl-1-naphthol (**4u**, 28% ee and **4v**, 54% ee). Finally, the 6-membered ring of the yne-enone **1a** could be replaced by a 7-membered ring, giving the bicyclic furane **4w** in 91% yield and 81% ee.

In summary, we have shown that the tandem cycloisomerization/nucleophilic addition reactions between 2-alkynyl enones **1** and ortho-substituted naphthols are efficiently catalyzed by CPAPhosAuCl complexes at low 0.2 mol % catalyst loadings. The bifunctional nature of the catalysts may result in a number of competing pathways resulting in structural and/or confugurational instability. The fine understanding of the mechanistic pathways at stake provided by both experimental and computational studies have been critical to develop an efficient method that proceeds without the racemization and skeletal instability that were limiting our previous endeavours. Many of the naphthols engaged in this study hence produced highly enantioenriched bicyclic furans under remarkably low catalytic loadings.

Experimental Section

Representative procedure: An oven-dried flask was charged with anhydrous solvent (1 mL), Au(I) catalyst (0.2 mol%) 2-alkynyl enones **1** (0.6 mmol, 1.5 equiv) and substituted naphthols **2** (0.4 mmol, 1 equiv) were added. Then, the reaction was kept stirring at 0 °C, under argon and the conversion was monitored by TLC. After 3-24 h, the solvent was removed under vacuum and the crude mixture purified on silica gel column chromatography (0% to 10% EtOAc/ petroleum ether), to afford compounds **4c-w**.
Note: for reactions carried out with the Ag_2CO_3 co-catalyst, the silver salt (0.1 mol%) wad added to the Au(I) catalyst before addition of the starting materials and the mixture was stirred for 15 min at rt.
Representative compound: (*S*)-4-((1,3-dimethylnaphthalen-2-yl)oxy)-2-phenyl-4,5,6,7-tetrahydrobenzofuran (4c). 4c was obtained from **1a** (118 mg, 0.6 mmol), **2c** (69 mg, 0.4 mmol) and catalyst **3b** (0.86 mg, 0.0008 mmol, 0.2 mol%) after 5 h at 0°C. Compound **4c** was isolated as a yellow solid (137 mg, 0.37 mmol, 93% yield). ^{1}H NMR (500 MHz, $CDCl_3$) δ 7.91 (d, *J* = 8.3 Hz, 1H), 7.73 (d, *J* = 8.0 Hz, 1H), 7.52 – 7.50 (m, 3H), 7.44 (t, *J* = 7.8 Hz, 1H), 7.39 (t, *J* = 7.3 Hz, 1H), 7.30 (t, *J* = 7.5 Hz, 2H), 7.19 (t, *J* = 7.3 Hz, 1H), 6.19 (s, 1H), 4.98 (t, *J* = 3.6 Hz, 1H), 2.89 – 2.84 (m, 1H), 2.70 – 2.64 (m, 1H), 2.58 (s, 3H), 2.40 (s, 3H), 2.38 – 2.30 (m, 1H), 2.27 – 2.24 (m, 1H), 1.98 – 1.95 (m, 1H), 1.87 – 1.81 (m, 1H). ^{13}C NMR (125 MHz, $CDCl_3$) δ 153.5, 153.0, 152.5, 132.9, 132.1, 131.2, 131.0, 128.8, 127.8, 127.7, 127.1, 125.3, 125.2, 124.6, 124.1, 123.7, 119.7, 105.4, 74.2, 29.8, 23.6, 19.3, 18.3, 13.0. HRMS calcd for $C_{26}H_{25}O_3$ $[M+O+H]^+$: 385.1798, found: 385.1802; $[\alpha]_D$ = -239.0 (*c* 1.00, $CHCl_3$); HPLC Analysis: 95% ee [©Chiralpak IB, 25 °C, 5% *i*PrOH/*n*-heptane, 1 mL/min, 280 nm, retention times: 4.3 min (major) and 4.7 min (minor)].

Acknowledgements

This work has been supported in part by the ANR funding agency via the collaborative project "BiAuCat" (ANR-20-CE07-0037). We thank the China Scholarship Council for PhD funding to Y. Y. and Z. Z., the ANR for the Post-doctoral fellowship to N.S. and PhD fellowship of M. D. and the GDR Phosphore for support.

References

[1] a) D. Qian, J. Zhang, *Acc. Chem. Res.* **2020**, *53*, 2358; b) X. Bao, J. Ren, Y. Yang, X. Ye, B. Wang, H. Wang, *Org. Biomol. Chem.* **2020**, *18*, 7977; c) D. B. Huple, S. Ghorpade, R.-S. Liu, *Adv. Synth. Catal.* **2016**, *358*, 1348; d) A. L. Siva Kumari, A. Siva Reddy, K. C. K. Swamy, *Org. Biomol. Chem.* **2016**, *14*, 6651; e) D. Qian, J. Zhang, *Chem. Rec.* **2014**, *14*, 280.

[2] a) T. Yao, X. Zhang, R. C. Larock, *J. Org. Chem.* **2005**, *70*, 7679; b) T. L. Yao, X. X. Zhang, R. C. Larock, *J. Am. Chem. Soc.* **2004**, *126*, 11164.

[3] a) S. Liu, P. Yang, S. Peng, C. Zhu, S. Cao, J. Li, J. Sun, *Chem. Commun.* **2017**, *53*, 1152; b) Y. Zheng, Y. Chi, M. Bao, L. Qiu, X. Xu, *J. Org. Chem.* **2017**, *82*, 2129; c) Y. Wang, P. Zhang, D. Qian, J. Zhang, *Angew. Chem. Int. Ed.* **2015**, *54*, 14849; d) Y. Wang, Z.-M. Zhang, F. Liu, Y. He, J. Zhang, *Org. Lett.* **2018**, *20*, 6403; e) F. Liu, Y. Yu, J. Zhang, *Angew. Chem. Int. Ed.* **2009**, *48*, 5505; f) F. Liu,

D. Qian, L. Li, X. Zhao, J. Zhang, *Angew. Chem. Int. Ed.* **2010**, *49*, 6669; g) Z.-M. Zhang, P. Chen, W. Li, Y. Niu, X.-L. Zhao, J. Zhang, *Angew. Chem. Int. Ed.* **2014**, *53*, 4350.

[4] For examples, see: a) C. H. Oh, V. R. Reddy, A. Kim, C. Y. Rhim, *Tetrahedron Lett.* **2006**, *47*, 5307; b) Y. Xiao, J. Zhang, *Angew. Chem. Int. Ed.* **2008**, *47*, 1903; c) R. Liu, J. Zhang, *Chem. Eur. J.* **2009**, *15*, 9303; d) Y. Xiao, J. Zhang, *Adv. Synth. Catal.* **2009**, *351*, 617; e) W. Li, J. Zhang, *Chem. Commun.* **2010**, *46*, 8839; f) G. Force, Y. L. T. Ki, K. Isaac, P. Retailleau, A. Marinetti, J. F. Betzer, *Adv. Synth. Catal.* **2018**, *360*, 3356; g) N. T. Patil, H. Y. Wu, Y. Yamamoto, *J. Org. Chem.* **2005**, *70*, 4531; h) V. Rauniyar, Z. J. Wang, H. E. Burks, F. D. Toste, *J. Am. Chem. Soc.* **2011**, *133*, 8486; i) L. Huang, F. Hu, Q. Ma, Y. Hu, *Tetrahedron Lett.* **2013**, *54*, 3410; j) S. R. Pathipati, A. van der Werf, L. Eriksson, N. Selander, *Angew. Chem. Int. Ed.* **2016**, *55*, 11863; k) X. Liu, Z. Pan, X. Shu, X. Duan, Y. Liang, *Synlett* **2006**, 1962; l) J. Qi, Q. Teng, N. Thirupathi, C.-H. Tung, Z. Xu, *Org. Lett.* **2019**, *21*, 692.

[5] For initial reports, see: a) S. Mayer, B. List, *Angew. Chem. Int. Ed.* **2006**, *45*, 4193; b) M. Mahlau, B. List, *Angew. Chem. Int. Ed.* **2013**, *52*, 518; c) G. L. Hamilton, E. J. Kang, M. Mba, F. D. Toste, *Science* **2007**, *317*, 496; d) S. Mukherjee, B. List, *J. Am. Chem. Soc.* **2007**, *129*, 11336.

[6] For reviews about enantioselective Au(I)-catalysis, see: a) S. Sengupta, X. Shi, *ChemCatChem* **2010**, *2*, 609; b) A. Pradal, P. Y. Toullec, V. Michelet, *Synthesis* **2011**, 1501; c) G. Cera, M. Bandini, *Isr. J. Chem.* **2013**, *53*, 848; d) Y.-M. Wang, A. D. Lackner, F. D. Toste, *Acc. Chem. Res.* **2014**, *47*, 889; e) W. Zi, D. F. Toste, *Chem. Soc. Rev.* **2016**, *45*, 4567; f) Y. Li, W. Li, J. Zhang, *Chem. Eur. J.* **2017**, *23*, 467.

[7] a) Z. Zhang, V. Smal, P. Retailleau, A. Voituriez, G. Frison, A. Marinetti, X. Guinchard, *J. Am. Chem. Soc.* **2020**, *142*, 3797; b) Y. Yu, Z. Zhang, A. Voituriez, N. Rabasso, G. Frison, A. Marinetti, X. Guinchard, *Chem. Commun.* **2021**, *57*, 10779; c) Z. Zhang, N. Sabat, G. Frison, A. Marinetti, X. Guinchard, *ACS Catal.* **2022**, *12*, 4046; d) Y. Yu, N. Sabat, M. Daghmoum, Z. Zhang, P. Retailleau, G. Frison, A. Marinetti, X. Guinchard, *Org. Chem. Front.* **2023**, *10*, 2936.

[8] For a related approach, see: À. Martí, M. Montesinos-Magraner, A. M. Echavarren, A. Franchino, *Eur. J. Org. Chem.* **2022**, *2022*, e202200518.

[9] Z. Li, J. Peng, C. He, J. Xu, H. Ren, *Org. Lett.* **2020**, *22*, 5768.

[10] T. Pielhop, G. Larrazábal, P. Rudolf von Rohr, *Green Chem.* **2016**, *18*, 5239.

[11] Effects of counter-ions in Au(I) catalysis, see: a) Z. Lu, T. Li, S. R. Mudshinge, B. Xu, G. B. Hammond, *Chem. Rev.* **2021**, *121*, 8452; b) Z. Lu, G. B. Hammond, B. Xu, *Acc. Chem. Res.* **2019**, *52*, 1275; c) J. Schiessl, J. Schulmeister, A. Doppiu, E. Woerner, M. Rudolph, R. Karch, A. S. K. Hashmi, *Adv. Synth. Catal.* **2018**, *360*, 2493; d) J. Schießl, J. Schulmeister, A. Doppiu, E. Wörner, M. Rudolph, R. Karch, A. S. K. Hashmi, *Adv. Synth. Catal.* **2018**, *360*, 3949; e) Z. Lu, J. Han, O. E. Okoromoba, N. Shimizu, H. Amii, C. F. Tormena, G. B. Hammond, B. Xu, *Org. Lett.* **2017**, *19*, 5848; f) F. Jaroschik, A. Simonneau, G. Lemiere, K. Cariou, N. Agenet, H. Amouri, C. Aubert, J.-P. Goddard, D. Lesage, M. Malacria, Y. Gimbert, V. Gandon, L. Fensterbank, *ACS Catal.* **2016**, *6*, 5146; g) M. Jia, M. Bandini, *ACS Catal.* **2015**, *5*, 1638.

[12] Effects of the silver salt in Au(I) catalysis, see: a) A. Zhdanko, M. E. Maier, *ACS Catal.* **2015**, *5*, 5994; b) B. Ranieri, I. Escofet, A. M. Echavarren, *Org. Biomol. Chem.* **2015**, *13*, 7103; c) A. Homs, I. Escofet, A. M. Echavarren, *Org. Lett.* **2013**, *15*, 5782; d) D. Wang, R. Cai, S. Sharma, J. Jirak, S. K. Thummanapelli, N. G. Akhmedov, H. Zhang, X. Liu, J. L. Petersen, X. Shi, *J. Am. Chem. Soc.* **2012**, *134*, 9012; e) D. Weber, M. R. Gagné, *Org. Lett.* **2009**, *11*, 4962.

[13] For reviews about the development of silver-free strategies in Au(I) catalysis, see: a) A. Franchino, M. Montesinos-Magraner, A. M. Echavarren, *Bull. Chem. Soc. Jpn.* **2021**, *94*, 1099; b) S. Gaillard, J. Bosson, R. S. Ramón, P. Nun, A. M. Z. Slawin, S. P. Nolan, *Chem. Eur. J.* **2010**, *16*, 13729; c) H. Schmidbaur, A. Schier, *Z. Naturforsch. B* **2011**, *66*, 329.

[14] For recent examples of silver-free strategies in Au(I) catalysis, see: a) P. Elías-Rodríguez, E. Matador, M. Benítez, T. Tejero, E. Díez, R. Fernández, P. Merino, D. Monge, J. M. Lassaletta, *J. Org. Chem.* **2023**, *88*, 2487; b) A. M. Echavarren, A. Franchino, À. Martí, S. Nejrotti, *Chem. Eur. J.* **2021**, *27*, 11989; c) S. Sen, F. P. Gabbaï, *Chem. Commun.* **2017**, *53*, 13356; d) O. Seppänen, S. Aikonen, M. Muuronen, C. Alamillo-Ferrer, J. Burés, J. Helaja, *Chem. Commun.* **2020**, *56*, 14697; e) A. Guérinot, W. Fang, M. Sircoglou, C. Bour, S. Bezzenine-Lafollée, V. Gandon, *Angew. Chem. Int. Ed.* **2013**, *52*, 5848; f) H. F. Jónsson, D. Sethio, J. Wolf, S. M. Huber, A. Fiksdahl, M. Erdelyi, *ACS Catal.* **2022**, *12*, 7210.

[15] Furthermore, we assume that a similar reaction pathway occurs from pro-(*R*)-**8a** to account for the experimentally observed formation of (*R*)-**5a**, although this has not been calculated.